energies

MDPI

Article

Communication-Less Data-Driven Coordination Technique for Hybrid AC/DC Transmission Networks

Arif Mehdi [1], Syed Jarjees Ul Hassan [1], Zeeshan Haider [1], Ho-Young Kim [1] and Arif Hussain [2,*]

[1] Department of Electrical and Computer Engineering, Sungkyunkwan University, Suwon 16419, Republic of Korea; mehdiarif@skku.edu (A.M.); jarjess@skku.edu (S.J.U.H.); zeeshan776@skku.edu (Z.H.); rndud2906@skku.edu (H.-Y.K.)
[2] Electrical Engineering Department, Iowa University, Iowa City, IA 52242, USA
* Correspondence: hussain@iastate.edu

Abstract: There is a paradigm shift to hybrid (AC/DC) networks that integrate both AC and DC to meet growing energy demands, mitigate global warming, and interconnect distributed energy sources (DERs). However, the unique characteristics of AC/DC faults, the mutual interaction of hybrid lines, the harmonic components of converters/inverters, multiple directions of energy flow, and varying current levels have challenged the existing protection algorithms. Therefore, this paper presents a data-driven coordination AC/DC fault protection algorithm. The algorithm utilizes faulty voltage and current signals to retrieve the precise time-domain characteristics of AC, DC, and intersystem (IS) faults to develop the algorithm. The proposed algorithm consists of four stages: stage 1 includes the detection of faults, stage 2 identifies the fault as either AC or DC, stage 3 classifies the respective AC and DC faults, and stage 4 locates the AC/DC fault precisely. The hybrid test system is developed in a MATLAB/Simulink environment, and the data-driven algorithm is trained and tested in Python. The extensive simulation results for multiple fault cases, either AC or DC, and the comparisons of various performance indicators confirm the effectiveness of the developed algorithm, which performs efficiently under a noisy and extended hybrid AC/DC network. Compared to other schemes, the proposed coordination protection approach can enhance the speed and accuracy of hybrid AC/DC networks.

Keywords: fault protection; AC/DC protection coordination; data-driven approach; intelligent fault protection; ensemble learning protection

Academic Editor: Ahmed Abu-Siada

Received: 10 February 2025
Revised: 9 March 2025
Accepted: 10 March 2025
Published: 13 March 2025

Citation: Mehdi, A.; Hassan, S.J.U.; Haider, Z.; Kim, H.-Y.; Hussain, A. Communication-Less Data-Driven Coordination Technique for Hybrid AC/DC Transmission Networks. *Energies* **2025**, *18*, 1416. https://doi.org/10.3390/en18061416

1. Introduction

AC transmission lines transmit huge amounts of energy to end-users from centralized sources with maximum limits. However, the capacity of existing AC lines will be depleted to satisfy rising energy demands [1]. The AC transmission network extension is now restricted due to environmental concerns, regulatory rules, and right-of-way limitations [2]. Decentralized distributed energy resources (RERs) are being deployed in power systems to meet emerging energy requirements and mitigate environmental concerns [3]. Moreover, compared to the commonly used high-voltage AC (HVAC) systems, high-voltage DC (HVDC) and hybrid AC/DC networks have garnered more consideration due to their effective land management, right-of-way minimization, high performance, and reliability [4,5]. Hybrid transmission allows for bulk power transmission [6], providing a continuous energy supply, and a green environment [7]. Consequently, it can be established on existing AC lines on the same tower with new DC lines added to run in parallel with the AC lines [8,9]. These are alternative options for satisfying rising energy demands by increasing capacity

and reducing transmission losses over long distances [10]. This uninterrupted energy supply, with high transmission capacity, makes the parallel hybrid AC/DC transmission system more reliable and secure, being able to overcome the existing challenges [11]. However, this integration has further increased the complexity and vulnerability of network control by introducing harmonics, different AC/DC fault natures, and multi-directional energy sources. Therefore, hybrid AC/DC network protection is becoming more susceptible to transient disturbances and faults [12]. A scheme was presented in [13] to protect AC lines using composite mode power difference. Similarly, another scheme is used to overcome the AC protection challenge using composite mode inductance for different fault zones [14]. Another scheme in [15] employed a protection solution for AC lines using the unique boundary condition of the negative sequence strategy at the fault location. These schemes have protection solutions for the AC side but cannot simultaneously apply to hybrid AC/DC faults.

Prompt identification and classification of transient events and both AC/DC faults are required to protect the transmission network [16]. The scheme used in [17] provides solutions for emerging cascading faults due to the interaction of hybrid lines. The simulation results demonstrated that initiating the fault from the AC inverter side leads to communication failure and DC system blockage. Integrated control schemes were presented in [18] to avoid the blackouts caused by cascading failures in hybrid transmission. Intersystem (IS) faults can originate due to short circuits of AC and DC lines in AC/DC transmission lines [19]. Several techniques were presented in [20] to overcome mutual interaction challenges and provide secure IS fault handling by using the protection coordination of AC/DC and full-bridge multilevel converters. A control strategy of bidirectional converters for transient response was proposed in [21] to overcome the faults in the hybrid system. A novel scheme in [22] used a transfer matrix to detect, locate, and identify hybrid line faults. However, the scheme has used samples from both ends of the line so it may cause communication failures. An algorithm of directional elements to overcome commutation failures in hybrid transmission lines was presented in [23]. This technique can face data mismatch errors during data collection. A full-bridge control mechanism to control the hybrid transmission line fault was proposed in [24]. Compared to the half-bridge control, the proposed scheme has solved the protection issues of both AC/DC sides. The challenges with control schemes are high computation, increased complexity, and cost.

Currently, machine learning methods have received much interest in detecting and diagnosing transmission line issues [25]. These technique's main benefits include fast detection, low complexity, and high accuracy for AC/DC faults in hybrid lines. Hence, they can prevent failure promptly and advance the dependability and robustness of the utilized systems. The support vector machine (SVM) algorithm [26] has been utilized to improve the safety of AC/DC faults. This technique uses a discrete Fourier transform for feature extraction to detect AC and HVDC faults. Another scheme was presented for the recognition and categorization of AC and DC fault lines using the k-nearest neighbor algorithm [27]. The technique used the discrete wavelet transform for the data and feature attributes to detect fault abnormality. In [28], a fault protection scheme using traveling waves was proposed. The scheme utilized the discrete wavelet transformation to detect the transient events of selected parameters with the SVM for fault identification. A reinforcement learning-based protection scheme for hybrid microgrids to optimize energy storage systems was presented in [29].

The existing literature mostly deals with the protection of HVDC networks using artificial neural networks (ANNs) with the discrete wavelet transform (DWT) to extract relevant features. DWT is used to derive important features and minimize noise and abnormal events. Feature selection to ensure the nature and timing of the faults plays a

main role in the ANN algorithms. Ant colony optimization has been employed in [30] to ensure optimal accuracy in fault protection by selecting only the optimized features. A robust ANN-based protection scheme for multi-terminal HVDC systems utilizes Bayesian optimization (BO) to fine-tune the parameters of the DWT. This method leverages multi-resolution analysis and Parseval's theorem to enhance parameter tuning, thereby improving the efficiency of internal DC fault detection [31]. Deep learning (DL) has been used for fault detection in DC networks. A transfer learning approach using adversarial DL was used to identify short-circuit faults, where transient line currents serve as input features for classification. This technique demonstrates a fast fault protection time of approximately 1 ms, making it highly effective for real-time applications [32]. A method based on the pi-line model has been proposed to determine fault locations within AC/DC microgrids. By analyzing voltage and current data at the point of common coupling and generator terminals, this approach accurately identifies fault location [33]. A single-phase ground fault detection strategy utilizes the whale optimization algorithm to optimize the parameters of least squares SVM, improving classification accuracy [34]. In microgrid protection, a hybrid approach combining the DWT with neural networks has been developed, leveraging the strengths of both techniques to enhance system reliability [35].

A unified mathematical-driven scheme [36] with the ability to coordinate the AC and DC relay impedances can detect both AC and DC faults. This algorithm has ensured the simultaneous detection of AC and DC faults as a single relay in a microgrid. The performance of the proposed algorithm can be varied during transient events owing to the impedance-based relays. Currently, no study deals with simultaneous hybrid transmission network AC/DC faults.

The existing schemes mostly deal with either HVDC or HVAC faults separately. The conventional schemes cannot protect the hybrid networks due to bidirectional power flow and complex control algorithms. Existing intelligent algorithms rely on signal processing schemes that require threshold criteria, time computation and neglect the coordination of relays to simultaneously detect both AC and DC faults in hybrid networks. Therefore, intelligent coordination techniques are needed to quickly and precisely detect, locate, and classify AC/DC faults.

1.1. Research Gap

To address these limitations, there is an urgent demand for protection algorithms that ensure the coordinated operation of AC and DC protection relays while promptly detecting both AC and DC faults in hybrid networks. The existing techniques, while effective, often rely on computationally expensive feature extraction methods such as the DWT and deep learning models, which increase processing time and complexity. A key research gap lies in developing a coordination-based data-driven algorithm that leverages a simple yet effective time domain to achieve fast, reliable, and computationally efficient fault detection and classification. The proposed technique avoids complex signal processing while ensuring real-time applicability, making it suitable for hybrid AC/DC networks.

1.2. Contribution and Paper Organization

This paper proposes a communication-less data-driven coordination technique for hybrid transmission networks. The scheme uses time-domain features to identify the hybrid line fault (AC, DC, IS) scenarios. The data cases collected are then used to train the proposed algorithm. Hybrid network modeling and feature extraction were performed in MATLAB 2022a/Simulink, while Python (3.7.16) was used for the development of the algorithm and training/testing of the data.

The main contributions of this study are as follows:

- A communication-less data-driven coordination algorithm for the hybrid AC/DC transmission line is proposed to avoid time delays.
- The proposed algorithm simultaneously detects, locates, and classifies all the existing fault scenarios (AC, DC, and IS) to ensure the stability and reliability of the system compared to existing methods where parallel hybrid network protection cases are not thoroughly studied.
- The proposed algorithm is independent of any threshold requirement. Fault detection, identification, classification, and location steps are comprehensively investigated using noisy data and an extended test system to assess performance.
- The developed hybrid (AC/DC) network system operates in parallel to overcome the existing energy demands and enhance capacity without extending new AC lines.
- Finally, to confirm the efficacy, a thorough comparison with the state-of-the-art techniques is conducted using various performance indicators such as accuracy, precision, recall, and F1 score.

The remainder of this paper is organized as follows. Section 2 presents the mathematical modeling and fault characteristics analysis. Section 3 provides theoretical details of ensemble learners and thoroughly describes the proposed protection scheme. Section 4 briefly describes the hybrid AC/DC network and feature extraction details. Section 5 presents the simulation results and discussions, and Section 6 concludes the paper.

2. Mathematical Modeling and Fault Characteristics Analysis

The fault characteristics of AC and DC in VSC-based HVDC networks are analyzed thoroughly using resistive–inductive–capacitive (RLC) circuitry to develop protection algorithms [37].

2.1. DC Fault Analysis

DC faults generally considered in the literature are pole-to-ground (PG) and pole-to-pole (PP). The DC fault is highly intense owing to the cable's capacitor discharge and line impedance. The VSC has three stages during a fault [38], which are shown in Figure 1 as follows.

2.1.1. Discharge of Capacitors

The current is discharged from the capacitor during a fault in the first stage and it results in a fast-rising current due to the charged capacitor and low impedance of the cable, as shown in Figure 1a.

2.1.2. Freewheeling Diodes

In the later stage after discharging the capacitor, the voltage drops to zero, acting in reverse, pushing the freewheeling diodes (D) to start the conducting path, as shown in Figure 1b, where D is the diode of the converter leg.

2.1.3. Grid Feed

In Figure 1c, the AC feed stage, the current from the V_{grid} is introduced as i_{grid} along with capacitor i_c and inductor current i_L.

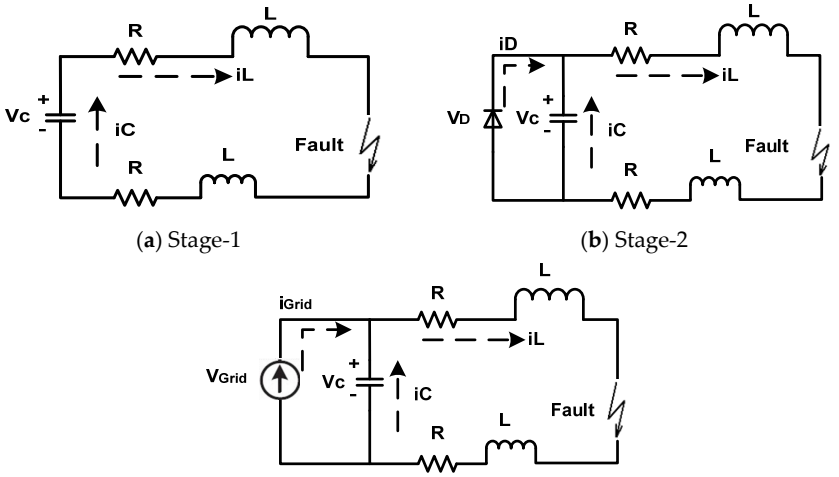

Figure 1. DC fault scenarios in VSC: (**a**) discharge of capacitor stage, (**b**) freewheeling diodes stage, (**c**) and AC feed stage.

The VSC fault current $i(t)$ used for the given networks to detect the abnormality is derived as follows:

$$i(t) = \frac{v_C(0)}{L(p_2 - p_1)}\left[e^{-p_1 t} - e^{-p_2 t}\right] + \frac{i_l(0)}{(p_2 - p_1)}\left[-p_1 e^{-p_1 t} - p_2 e^{-p_2 t}\right] \quad (1)$$

Here, p_1 and p_2 are the poles and are determined by the following:

$$p_1, p_2 = \alpha \pm \sqrt{(\alpha)^2 - {\omega_0}^2} \quad (2)$$

where $\omega_0 = \frac{1}{\sqrt{LC}}$ and $\alpha = \frac{R}{2L}$; the values may be real or complex. The fault (i_f) and diode currents (i_D) of the VSC are derived using (3):

$$i_f = {I'}_0 e^{-(\frac{R}{L})t} \text{ and } i_D = \frac{i_f}{3} \quad (3)$$

where ${I'}_0$ is the start value of the fault.

2.2. AC Fault Details

The fault behavior of AC faults is studied using a resistive–inductive (RL)-equivalent circuit, as shown in Figure 2 [39]. The switch initiates a fault and short circuits the load with low impedance, resulting in a high current level from the source. The fault current has an impedance calculated from the circuit using $(R + jX_L)$.

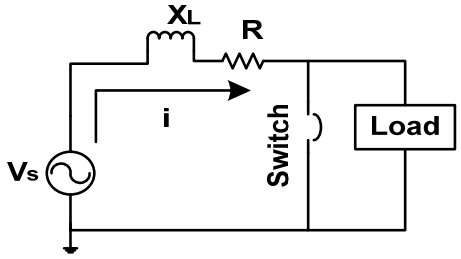

Figure 2. Circuit for fault current.

The AC fault current is studied when the switch is closed in Figure 2.

$$V_s = Ri + L\frac{di}{dt} \quad (4)$$

The fault currents are the combination of two components, as shown in (5), and can be determined by

$$i_{ac} = \frac{V_s}{R}\left(1 - e^{-\left(\frac{t}{T}\right)}\right),\ i_{dc} = I_0 e^{-\left(\frac{t}{T}\right)}. \quad (5)$$

The total sum of the AC fault current, including AC and DC being offset, is given as

$$i_{total} = i_{ac} + i_{dc} = \frac{V_s}{R} + \left(I_0 - \frac{V_s}{R}\right)e^{-\left(\frac{t}{T}\right)}. \quad (6)$$

These fault current characteristics are used to identify AC/DC faults and time-domain features are retrieved to detect the abnormality using data-driven approaches.

3. Theoretical Details of Data-Driven Algorithm

3.1. Ensemble Learners

Machine learning-based intelligent fault detection and protection approaches have enhanced power system protection. Researchers have presented numerous ensemble learning-based approaches to detect faults in AC protection in recent years using bulk data [40]. The advantages of using ensemble methods are quite remarkable. The predicted accuracy is greater, bias and variance may be decreased, and most of the time, the model is not under/overfitted. It is more reliable, has less noise, and works fine with linear and non-linear types of data. However, there remains a gap in applying such data-driven schemes to hybrid protection to ensure safety and overcome growing energy demands. To overcome this, we employed two models to precisely detect, identify, locate, and accurately classify the faults in a hybrid AC/DC system. The working principles of the utilized models are discussed below.

3.1.1. Random Forest (RF)

Ensemble models are effective for reducing the overfitting in the decision tree. Being an ensemble model, RF uses a bunch of trees to overcome this issue. RF is an ensemble-based model that uses multiple decision trees. During the process of classification, each tree has an output, and the final classification is based on the majority output decision of the trees. Owing to its high accuracy and generalization performance, an emerging RF ensemble algorithm was investigated for fault protection [41]. Figure 3 shows the flow chart of the working principle of random forest. It reviews the working methodology and how it attains the final output decision based on the voting of multiple trees. The pseudo-code of the RF algorithm is given in Table 1. The scheme considers random samples from the dataset and randomly develops the decision trees. After voting on the decision trees, the tree with the most votes is selected.

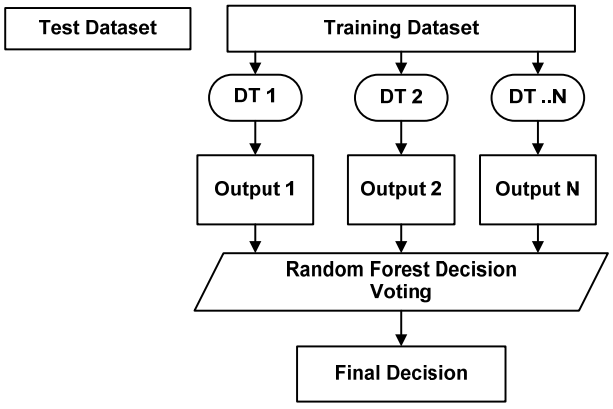

Figure 3. Flowchart of RF algorithm.

Table 1. RF algorithm [42].

RF Algorithm for Classification
1: For b = 1 to B:
A. From the training data, create a bootstrap of sample $z*$ of size N.
B. Recursively repeat the following procedures for each terminal node of the tree until the minimal node size n_{min} is attained, to generate an RF tree T_b from the bootstrapped data.
• From the p variables, choose m variables at random.
• Choose the best variable/split-point from the m options.
• Divide the node into two daughter nodes.
2: The ensemble of trees should be output as $\{T_b\}_1^B$.
To build a predictive model at a new point x,
Classification: Let $\hat{C}_b(x)$ be the b^{th} RF tree's class prediction.
Then, $\hat{C}B_{rf}(x)$ =Majority vote $\{\hat{C}_b(x)\}_1^B$.
End

3.1.2. Gradient Boosting (GB)

Friedman introduced GB, which is an ensemble learning model for classification and regression. It can produce an effective model consisting of weak learners, such as decision trees. The core idea of GB is to optimize an objective arbitrary loss function to create and generalize the ensemble model in multiple stages [43]. The working principle of GB is described in Figure 4. It depicts how it improves the final output using multiple stages and how data are randomly split across subtrees to minimize the error of the loss function. After several steps, the loss function is minimized. Finally, the improved model is obtained.

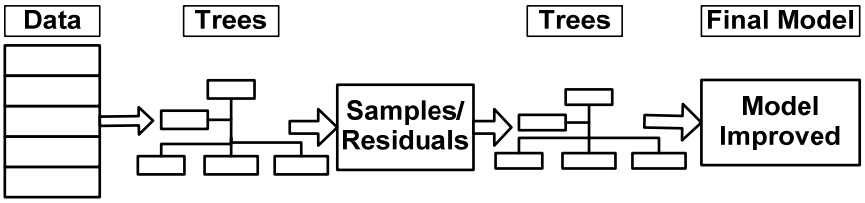

Figure 4. Detailed schematics of GB.

The advantage of using GB is the optimization of the loss function through iterative steps. The algorithm steps are presented in Table 2.

Table 2. GB algorithm [43].

Friedman's GB Algorithm
Inputs:
• Dataset $(x, y)_{i=1}^N$
• Iteration level M
• Selection of loss-function $\varphi(y, f)$
• Model base-learner selection $h(x, \varnothing)$
Algorithm:
1. Initialization with a constant $\hat{f}_0$
2. For $t = 1$ to M do
3. Calculate negative gradient $g_t(x)$
4. Adjust base-learner function $h(x, \varnothing_t)$
5. Adjust gradient-descent step size ρ_t : $\rho_t = \text{arg}min_\rho \sum_{i=1}^N \varphi\left[y_i,\ \hat{f}_{t-1}(x_i) + \rho h(x_i,\ \theta_t)\right]$
6. Function estimation updates: $\hat{f}_t \leftarrow \hat{f}_{t-1} + \rho_t h(x, \theta_t)$
7. End for

4. Proposed Data-Driven Coordination Protection Technique

The proposed technique employs the retrieved voltage and current signals. Accordingly, the most sensitive time-domain features are extracted to detect abnormality during faults. The features are selected to ensure all possible fault scenarios in a hybrid transmission line and train the algorithm to assess performance using testing data. The model operates in four stages: (1) detection of a fault, the algorithm is trained on the fault, and no-fault data. The first stage ensures the detection of faults successfully from the transient events, (2) identification of either an AC or DC fault, after fault detection, the fault is identified whether on AC or DC line, (3) classification of the respective fault, after identification of the respective faults is classified either AC or DC and (4) fault location estimation. Finally, the algorithm locates the fault on the line. An overview of the proposed data-driven protection algorithm for a hybrid transmission network is shown in Figure 5.

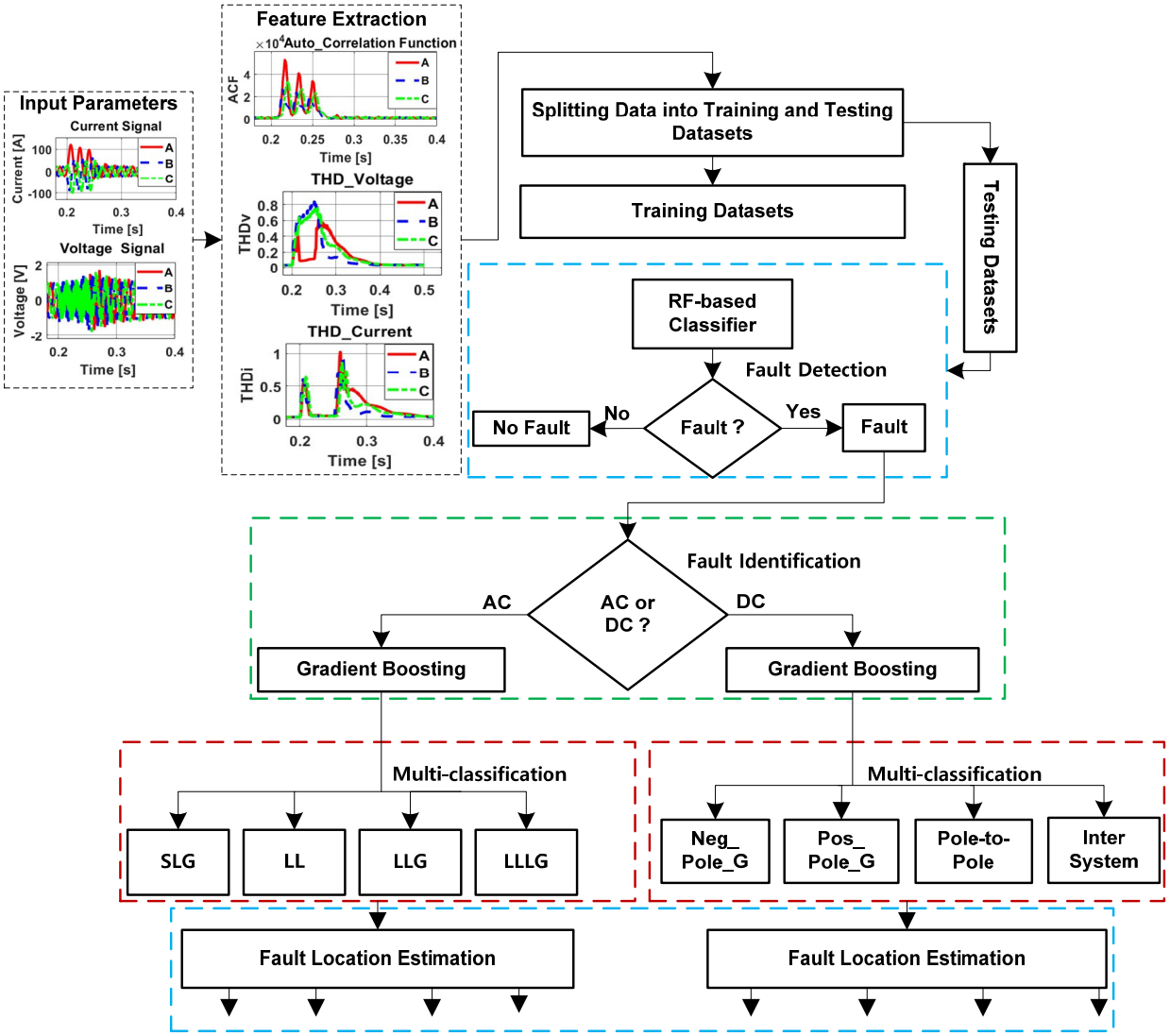

Figure 5. Flowchart of proposed fault detection and classification scheme.

5. Details of Hybrid Network and Feature Extraction

5.1. Hybrid AC/DC Network

The test system for the proposed protection algorithm was designed in a MATLAB/Simulink environment, as shown in Figure 6. The single-line diagram of the system includes hybrid AC/DC parallel lines on the same tower. The hybrid transmission network

consists of two parallel lines, a 765-kV AC line, and a 230-kV DC line, both of which are 200 km long and transfer 3000 MW of power from a generating source of 12 350-MVA generators to a source with a 20-GVA short-circuit level. A 13.8 kV/765 kV Wye-Delta transformer connects the system to the AC transmission line, while a 765 kV/230 kV Wye-Delta transformer connects it to the DC lines. The parameter lines of the models are distributed. The lines are meant to be transposed, with positive and zero-sequence components for the R, L, and C/km parameters. A forced commutated voltage source converter (VSC) connector is utilized in the DC line to transmit power. Three-level neutral-point clamped VSCs with near-insulated-gate bipolar transistor diodes are used in the rectifier and inverter. The proposed hybrid transmission line is shown in Figure 6, and the details are given in Appendix A.

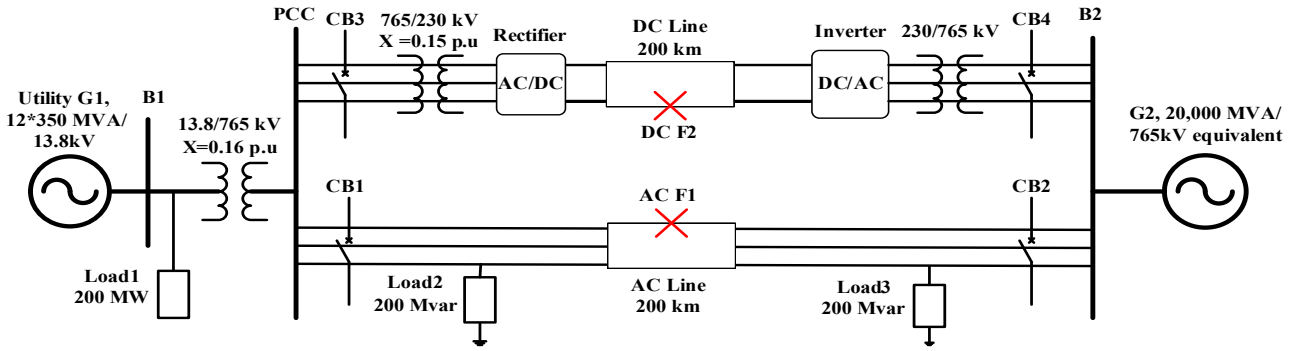

Figure 6. Proposed hybrid test system.

5.1.1. Fault Analysis

Fault analysis is performed to assess the nature of faults in the given hybrid system. The analysis of individual and corresponding faults highlights the associated challenges. The fault analysis results and challenges of the respective faults presented in the AC/DC and IS details are shown in Figures 7 and 8. Therefore, a robust protection mechanism is needed to resolve the issues of AC/DC faults in transmission systems.

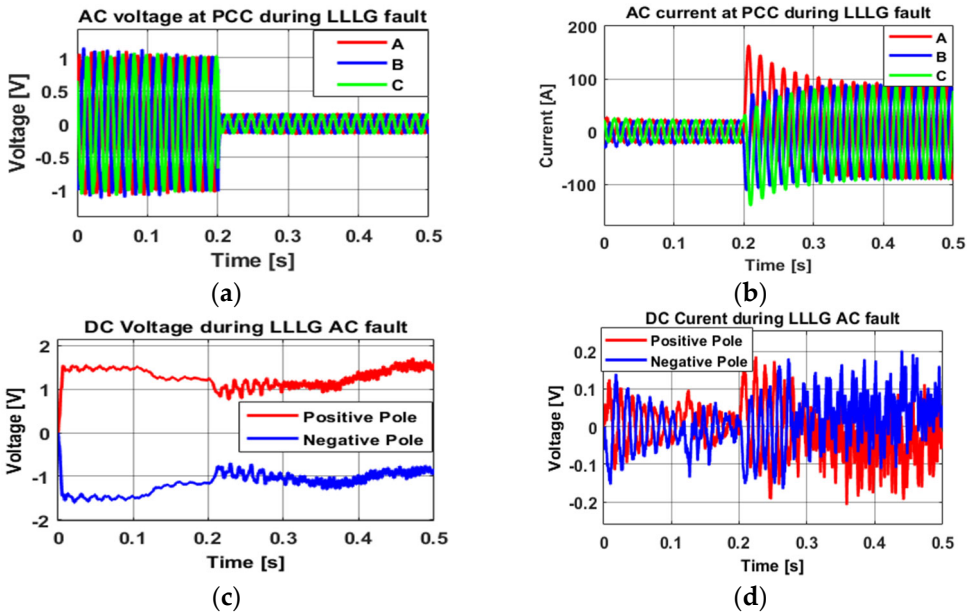

Figure 7. Fault scenarios: (**a**) the voltage of AC, (**b**) the current of AC, (**c**) the voltage of DC, and (**d**) the current of DC during an LLLG fault in the AC line of the hybrid test system.

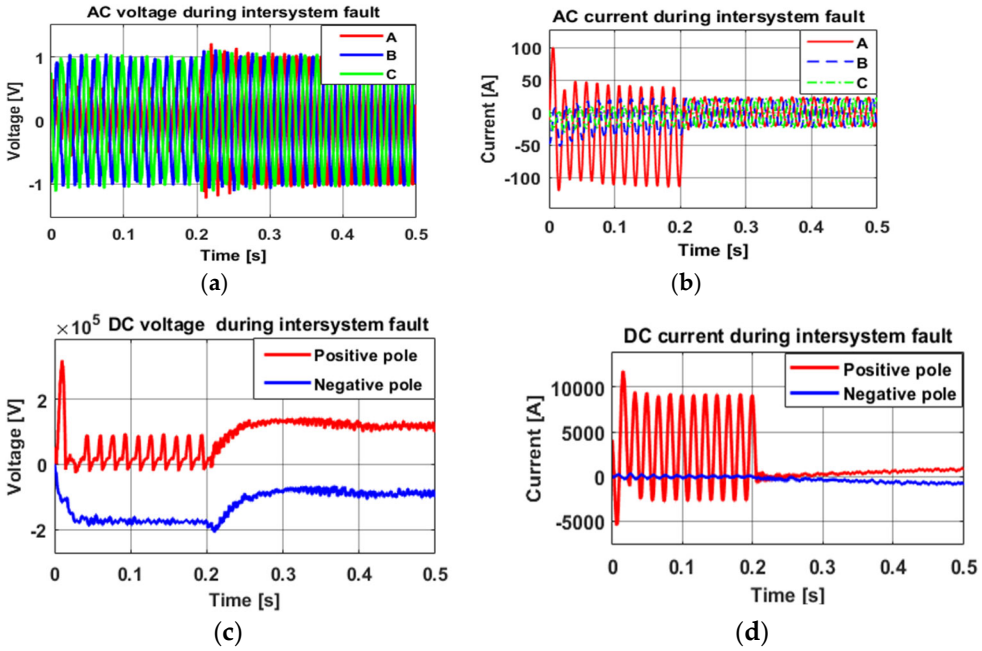

Figure 8. Fault scenarios: (**a**) the voltage of AC, (**b**) the current of AC, (**c**) the voltage of DC, and (**d**) the current of DC during an intersystem fault in the hybrid test system.

5.1.2. Fault Data Generation

To verify the efficacy of the proposed scheme, the hybrid test system is extensively investigated, as shown in Figure 6. Details regarding the collected data for faults (AC, DC, and intersystem) and no-fault scenarios in the designed model are presented in Tables 3 and 4.

Table 3. Parameters of unfaulty conditions.

Parameter Details	Counts
Abrupt load changes	10
Capacitor switching at PCC	20

Table 4. Parameters of simulated faulty conditions.

Parameter Details	Fault Events	Counts
Fault types	AC: LG, LL, LLG, LLLG DC: Pos. PG, Neg. PG, PP Intersystem: DC to AC	8
Fault resistance (Ω)	0.1 to 90	10
Fault inception angle (°)	0, 45, 90, 270	4
Different locations (km)	25 to 175	7

The no-fault scenarios are created by changing the abrupt loads and using capacitor switching to create transient events. These transient events are not considered faulty, so we can assess the proposed algorithm's ability to differentiate between the fault and transient events. The eight types of faults are: four types of AC faults (LG, LL, LLG, LLLG), three types of DC faults (Pos. PG, Neg. PG, PP), and an intersystem fault (DC pole to AC line).

5.1.3. Details of Feature Extraction and Behaviors of Selected Features

The existing schemes utilize signal processing techniques that need high computation and specific thresholds to detect the faults. To overcome this gap, the proposed approach considers sensitive and feasible time-domain features of hybrid fault scenarios to ensure

fault anomaly detection. Accurate and reliable detection of abnormalities requires the careful selection of feature parameters [44]. Hence, time-domain features can provide faster and more accurate protection while reducing complexity. The fault data are collected by variations in fault resistance, fault type, fault inception angle, and location. Conversely, the no-fault scenarios are achieved via abrupt load fluctuations and capacitor switching. After relevant features are extracted, the proposed algorithms are trained for AC, DC, and intersystem faults. Fault duration varies across intervals of 0.2 to 0.25 s. The details of the utilized features are shown in Table 5. Figure 9 provides an overview of the retrieved time-domain features. The standard deviation of selected features is used for data collection to ensure accurate and reliable detection of abnormalities. Feature extraction allows the models to execute their functions, and the sensitive features are selected to ensure a transient nature and irregularity during disturbance. This approach has significantly contributed to the performance of the developed algorithm and promptly detects faults and avoids network blackouts.

Table 5. Feature details of simulated faults.

Equation	Feature Detail
$r_k = \frac{\sum_{i=1}^{M-k}(x-x')(x_{i+k}-x')}{\sum_{i=1}^{M-k}(x-x')^2}$	where r_k represents the autocorrelation function, x_i represents the original dataset, x_{i+k} represents the shifted dataset, and the sample denoted by M and $x\prime$ represents the mean data point
$V_{rms} = \sqrt{\frac{\sum_{k=1}^{N} V_k 2}{N}}$ $I_{rms} = \sqrt{\frac{\sum_{k=1}^{N} I_k 2}{N}}$	The RMS value of current and voltage gives the variation in any distortion during abnormal action
$THD_V = \frac{\sqrt{V_2^2+V_3^2+V_4^2+...+V_n^2}}{V_1}$ $THD_i = \frac{\sqrt{I_2^2+I_3^2+I_4^2+...+I_n^2}}{I_1}$	THD_V represents the overall harmonic distortion of the voltages; THD_i represents the harmonic distortion of the current I_n
$E_T = \sum_{n=1}^{N} \left\| x(n)^2 \right\|$	The transient energy of the time-series voltage and current is computed using this formula, where E_T is the transient energy, $x(n)$ is the signal at index n, and N is the total number of samples

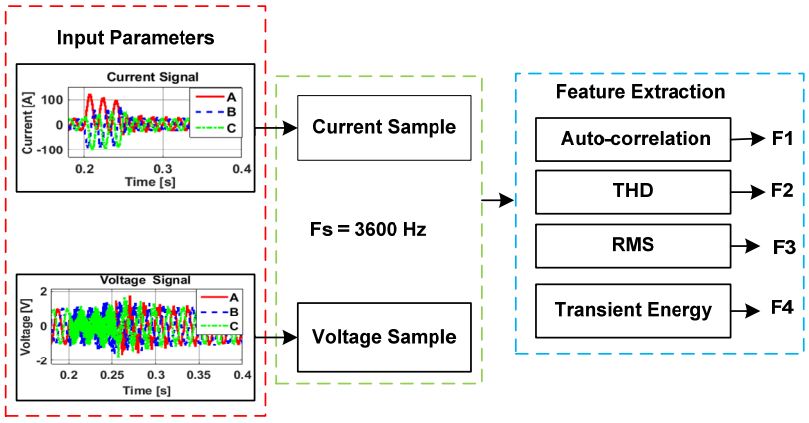

Figure 9. Feature extraction for the proposed scheme.

5.1.4. Fault Types and Behaviors of Selected Features

The behaviors of the retrieved voltages and currents are used to identify the distinct features of faults. When faults occur, the defective-phase voltage drops while the current rises in the given fault duration. Accordingly, the selected features of the faulty phase

vary compared with those of the healthy phases; therefore, according to these variations, it is easy to identify the faults. Owing to space limitations, only a few feature results are shown below. We investigated three types (AC, DC, and intersystem) of faults in the given test system. The voltage and current data retrieved from the given faults are shown in Figure 10a,b, and the extracted features (autocorrelation and THD) of the voltage and current are shown in Figure 10c–e, indicating the abnormality during the fault periods of 0.2 to 0.25 s. The faults due to the mutual interaction of AC and DC lines are called intersystem faults. The considered scenario of the fault is from the DC line to the AC line. The voltage, current, and extracted features during intersystem faults are shown in Figure 11. Signal distortion due to the nonlinear characteristics of the converters, complex control systems, and mutual interaction of the AC and DC lines are observed.

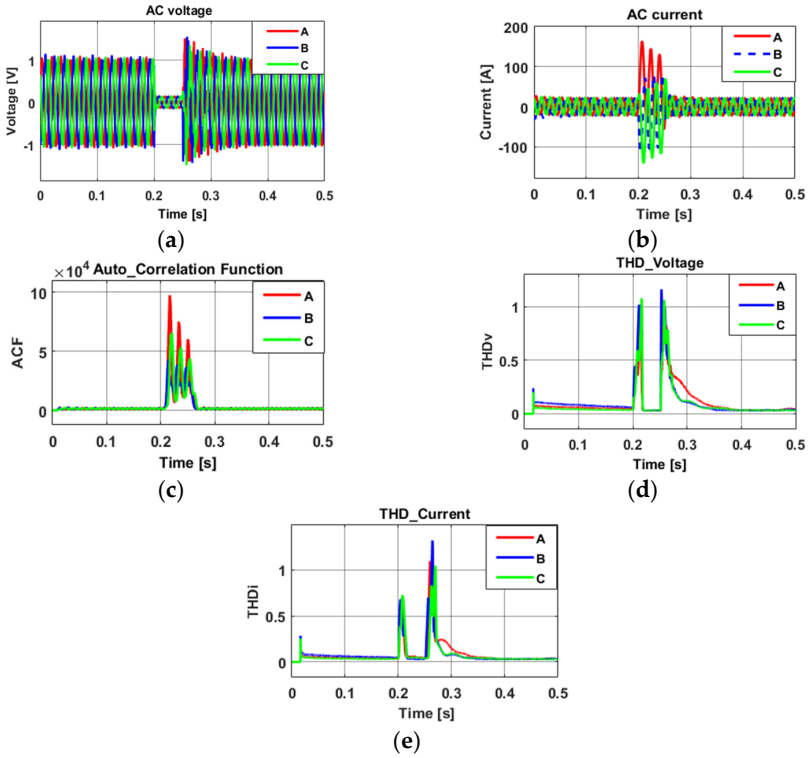

Figure 10. AC fault scenarios: (**a**) AC voltage, (**b**) AC current, (**c**) ACF of current, (**d**) THDv, and (**e**) THDi during LLLG faults.

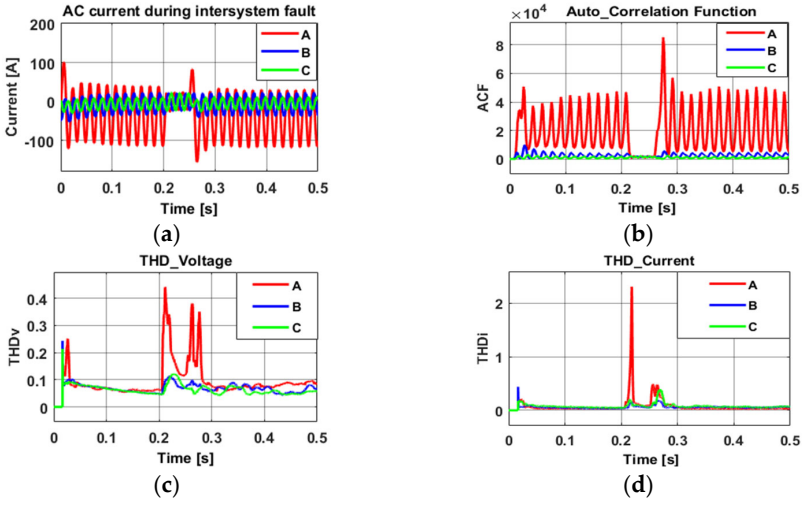

Figure 11. Intersystem fault scenarios: (**a**) AC current, (**b**) ACF of current, (**c**) THDv, and (**d**) THDi during intersystem fault.

6. Simulation Results and Discussion

To assess and compare the outcomes of the proposed data-driven algorithm, the following evaluation measures were used: accuracy (A), precision (P), and recall (R). These are the performance metrics used extensively in the field to evaluate and compare models. These are defined as follows:

$$\text{Accuracy} = \frac{\text{TP} + \text{TN}}{\text{TP} + \text{TN} + \text{FP} + \text{FN}} \tag{7}$$

$$\text{Precision} = \frac{\text{TP}}{\text{TP} + \text{FP}} \tag{8}$$

$$\text{Recall} = \frac{\text{TP}}{\text{TP} + \text{FN}} \tag{9}$$

Here, TP = true positive, TN = true negative, FP = false positive, and FN = false negative. Additionally, the confusion matrix was used to assess the algorithm's performance.

Fault location estimation is performed by using the regression GB model. The general function used to assess the performance of the regression model to optimize the location estimation error is calculated by using the mean square error (MSE), mean absolute error (MAE), and R^2, as follows:

$$MSE = \frac{\sum_{i=1}^{n} (D_{actual} - D_{est})^2}{n} \tag{10}$$

$$MAE = \frac{\sum_{i=1}^{n} |D_{actual} - D_{est}|}{n} \tag{11}$$

$$R^2 = 1 - \frac{n \times (MSE)^2}{\sum_{i=1}^{n} (D_{actual} - D_{est})^2} \tag{12}$$

The parameters for the MSE are D_{actual} and D_{est}, which are the actual and estimated fault distances, and n is the number of data samples for the model.

6.1. Performance Validation

6.1.1. Performance Analysis of Fault Detection and Identification Stage

The detection stage first determines the faulty and non-faulty cases to overcome the challenges of hybrid transmission faults. The RF model is used to detect faulty and unfaulty cases. The dataset is divided; 70% of the data is used to train the classifier and the remaining data (30%) tests model performance. The criteria for data division into training and testing sets are found in the existing literature. The dataset contains 200 no-fault cases and 880 fault cases. The fault and no-fault case scenarios are obtained, as shown in Tables 3 and 4. The tuning parameters used for this classifier are n_estimator, max-depth, and random_state. The feature details are given in Table 5. The performance of the model is presented in Table 6 using a confusion matrix. From the table, it can be seen that all 60 no-fault cases are classified correctly, and only 1 of the 264 fault cases is misclassified. The overall accuracy of the model is 99.69%, which is significantly higher than that of other classifiers, which strongly confirms the scheme's ability to detect faults accurately. The performance comparison with the DT and SVM in Figure 12a further strengthens the application of the model for fault detection.

After the detection of the fault, the next stage is to identify whether the fault is AC or DC. For this purpose, fault identification is performed using the RF on 440 AC and 440 DC cases (880). To ensure high performance, the dataset is divided into 70% training data and 30% testing data. The confusion matrix of the identification of faults is presented in Table 7, where all AC faults are classified accurately, and only one of the DC faults is misclassified. The accuracy of the AC and DC fault identification stage is 99.62%. The

overall performance of the proposed scheme is compared to other classifiers (DT and SVM) in terms of accuracy, precision, and recall, as shown in Figure 12b. The proposed algorithm outperforms other schemes in all three metrics.

Table 6. Confusion matrix for faulty and unfaulty cases.

Fault Type	NF	F
NF	60	0
F	1	263
Overall Accuracy (%)	99.69	

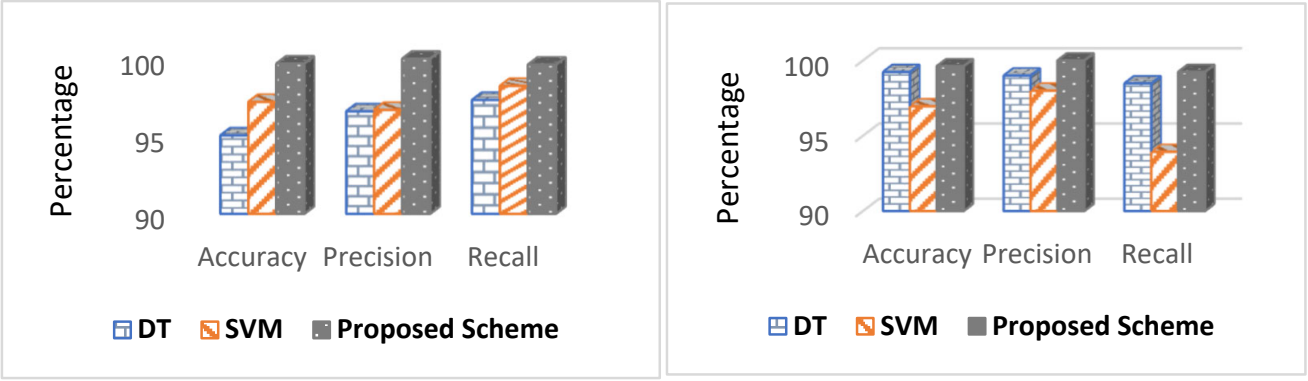

Figure 12. Performance comparison of the proposed detection and identification stages for (**a**) faulty/unfaulty scenarios and (**b**) AC/DC faults.

Table 7. Confusion matrix for AC and DC cases.

Fault Type	AC	DC
AC	132	0
DC	1	131
Overall Accuracy (%)	99.62	

6.1.2. Performance Analysis of AC and DC Fault Classification Stages

The proposed multi-fault scenarios considered are AC, DC, and intersystem faults. In this study, intersystem faults are considered DC faults to simplify the classification. After identification (AC or DC), the proposed algorithm utilizes ensemble learning-based GB to categorize the respective line faults. The algorithm designed for AC classification considers four types of faults: SLG, LL, LLG, and LLLG. The parameters used for GB are n-estimators, max-depth, and random-state. The performance of AC categorization using the confusion matrix is described in Table 8. During the classification, all the faults of LL and LLLG are classified correctly, whereas SLG has 1 and LLG has 2 faults misclassified. Hence, the overall accuracy is 97.72%. In the same way, for DC fault categorization, the scheme examines four faults: positive-pole–ground (Pos. PG), negative-pole–ground (Neg. PG), pole–pole (PP), and intersystem (IS, DC pole to AC line). The confusion matrix is presented in Table 9. The overall accuracy is 94.69%. The results indicate that five faults from Pos. PG and two from Neg. PG are misclassified, while PP and IS faults are correctly classified. A performance comparison of the multi-classification of the proposed algorithms based on accuracy, precision, and recall is presented in Figure 13. As seen, the proposed algorithm has higher accuracy compared to other classifiers. Hence, it is proven that the proposed algorithm offers an advantage over the alternatives in terms of classification.

Table 8. Confusion matrix for AC multi-classification.

Fault Type	SLG	LL	LLG	LLLG
SLG	32	0	1	0
LL	0	33	0	0
LLG	0	1	31	1
LLLG	0	0	0	33
Overall Accuracy (%)	97.72			

Table 9. Confusion matrix for DC multi-classification.

Fault Type	Pos_PG	Neg_PG	PP	IS
Pos_G	28	4	1	0
Neg_G	2	31	0	0
PP	0	0	33	0
IS	0	0	0	33
Overall Accuracy (%)	94.69			

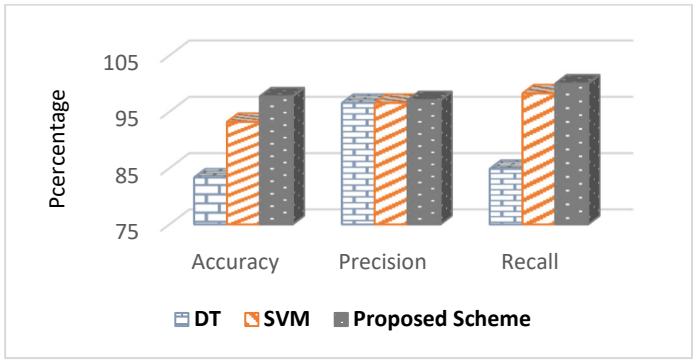

(**a**)

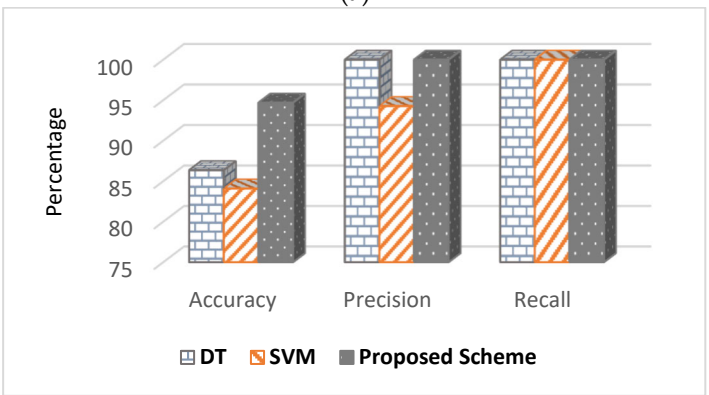

(**b**)

Figure 13. Performance comparison of the proposed multi-classification scheme for (**a**) AC multi-classification and (**b**) DC multi-classification.

6.1.3. Performance Analysis of Fault Location Estimation Stage

After fault detection and classification of respective faults, identifying the precise location of the fault is essential to prevent network disturbances. The gradient boosting (GB) regression model is used to estimate the fault location. The proposed model is trained to minimize the error in locating the faults precisely. The results show that the estimated location is close to the actual location of the faults. The minimum error further exemplifies the proposed model's ability to estimate fault location effectively. The performance metrics used to assess the regression models are derived in (10)–(12). The MSE for the

GB model has an optimum error and effectively estimates the actual fault locations. The RF regression model is compared with the proposed GB fault location estimation model to verify the performance metrics. The proposed GB fault location estimation method has efficiently estimated the performance metrics of the MSE (0.00659), AE (0.0613) and $R^2(0.999)$. The DC location estimation results for the given model are shown in Figure 14. Therefore, the proposed GB fault estimation efficiently estimates fault location in hybrid AC/DC networks.

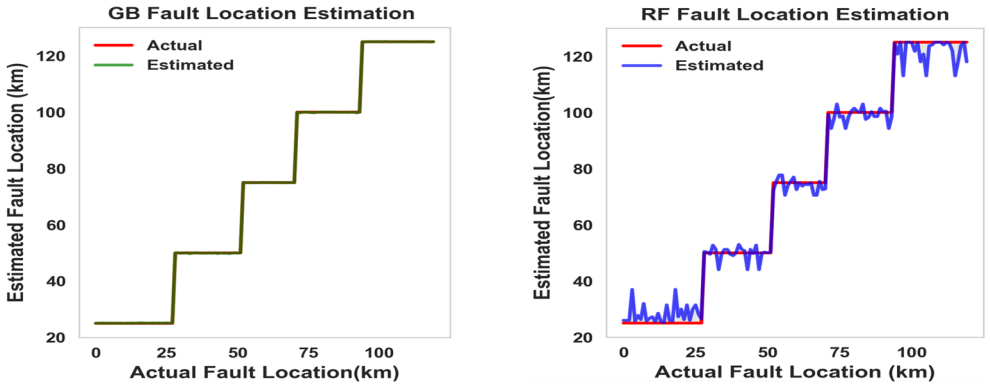

Figure 14. Performance analysis of fault location estimation models: (**a**) GB location estimation model and (**b**) RF location estimation model.

6.2. Performance Analysis with Noise

The proposed algorithm's immunity to noise was also investigated. To perform the simulations, the voltage and current measurements were distorted by the addition of noise with a 20 dB and 30 dB signal-to-noise ratio (SNR). The fault detection and binary classification steps using the proposed scheme were performed with the inclusion of noise. The robustness and performance of the proposed scheme have been maintained under the influence of noise, as shown in Table 10. Due to the ensemble architecture of the classifiers, it reliably works with noisy data. These findings strongly support employing ensemble learning models to overcome protection challenges in hybrid transmission lines.

Table 10. Influence of noise.

Technique	Methods	Noise Ratio	Accuracy %	Precision %	Recall %
Proposed Scheme	Fault detection	No noise	**99.69**	100	99.62
		30 dB	**98.76**	99.61	98.86
		20 dB	**97.53**	98.12	98.86
	Fault classification	No noise	**99.62**	100	99.24
		30 dB	**99.62**	100	99.24
		20 dB	**96.96**	97.69	96.21

6.3. Performance Evaluation on Extended Test System

The robustness and applicability of the proposed algorithm in existing systems has been thoroughly verified. Generally, existing machine learning-based protection algorithms merely assess performance on simple test systems. In this study, the hybrid test system shown in Figure 6 is extended to assess the proposed scheme's performance when multiple and complex AC and DC lines are operated. The new test system has three lines, one DC and two AC lines, as shown in Figure 15. Voltage and current data have been derived for AC, DC, and IS fault scenarios, as shown in Table 11. The total number of cases of AC and DC are 640, out of which 320 are AC and 320 are DC.

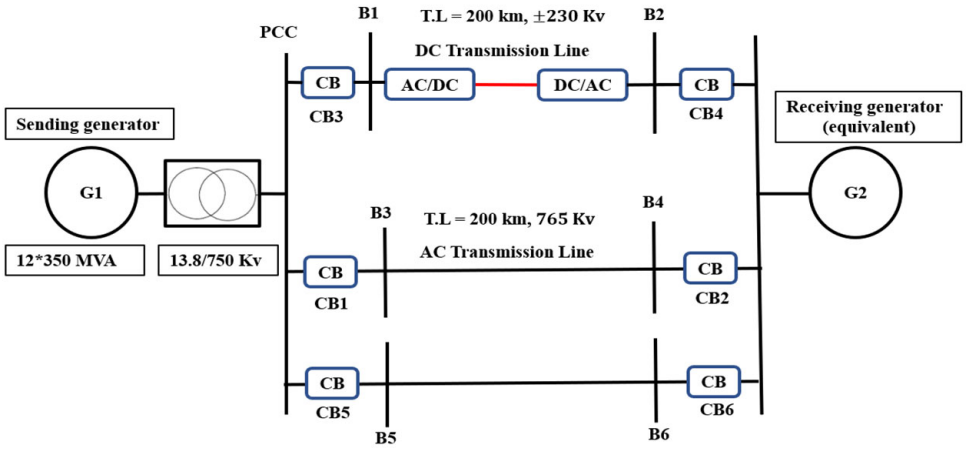

Figure 15. Extended proposed hybrid AC/DC test system.

Table 11. Parameters for simulated faulty conditions.

Parameter Details	Fault Events	Counts
Fault types	AC: LG, LL, LLG, LLLG DC: Pos. PG, Neg. PG, PP Intersystem: DC to AC	8
Fault resistance (Ω)	0.1 to 90	10
Fault inception angle (°)	0, 45, 90, 270	4
Different locations (km)	30 to 100	2

A confusion matrix offers a better representation of the proposed model's performance. Therefore, the data obtained from the extended system is utilized to verify the presented algorithm. The presented algorithm has performed well, as in the previous un-extended system.

Table 12 shows the algorithm's performance during the recognition of both AC/DC faults; the accuracy is 99.47%, while in the un-extended test system, it is 99.69%. Therefore, the presented algorithm is robust enough to apply in the extended complex network system.

Table 12. Confusion matrix for AC and DC cases.

Fault Type	AC	DC
AC	96	0
DC	1	95
Overall Accuracy (%)	99.47	

Similarly, the algorithm's performance is analyzed for the classification of faults in an extended system. The confusion matrix in Table 13 is for AC faults, while Table 14 shows the confusion matrix for DC faults. The accuracy of the proposed classification scheme for the extended system is almost the same as that for the un-extended test system for both AC and DC multi-classification.

Table 13. Confusion matrix for AC multi-classification.

Fault Type	SLG	LL	LLG	LLLG
SLG	24	0	0	0
LL	0	22	2	0
LLG	0	1	23	0
LLLG	0	0	0	24
Overall Accuracy (%)	96.87			

Table 14. Confusion matrix for DC multi-classification.

Fault Type	Pos_G	Neg_G	PP	IS
Pos_G	24	4	1	0
Neg_G	2	19	0	0
PP	0	0	24	0
IS	0	0	0	24
Overall Accuracy (%)	94.79			

The performance of the proposed algorithm has no specific effect as the system becomes more complicated in terms of the extra-linked transmission line. Therefore, the proposed algorithm can be applied to multi-terminal lines and for complex network protection.

Table 15 presents a comparison of the proposed scheme with existing schemes. The results indicate the importance of fault protection (AC, DC, and IS) in parallel AC/DC transmission networks utilizing the proposed data-driven algorithm. It has an advantage over others in terms of cost, complexity, and accuracy, and includes all faults of hybrid networks.

Table 15. Comparison with existing schemes.

Protection Method	Network Configuration	Complexity/Cost	Fault Studies	Accuracy/Time
[14] Pilot	Series	High/Normal	IF and EF	NR/NR
[18] Control	Parallel	Normal/Normal	Cascading	NR/500 ms
[20] Distance	Series	High/High	IS	NR/80 ms
[22] Pilot	AC Series	High/High	AC	NR/0.025 s
[25] ANN	MG	High/High	AC	NR/0.00058 s
[27] KNN	Series	Normal/Moderate	AC, DC	100%
Proposed Scheme	Parallel	Simple/Less	AC, DC, IS	AC = 99.69% DC = 99.62%

NR: not reported; IS: intersystem; IF: internal fault; EF: external fault; MG: microgrid.

6.4. Discussion and Future Directions

Hybrid transmission is an emerging field for power systems as it offers a solution to rising energy demands and environmental challenges. Traditional protection methods only address a specific type of fault, such as AC, DC, or IS. This paper has proposed an algorithm to timely remove the transient events and detect, identify, locate, and classify all faults that may occur in parallel hybrid transmission. The algorithm proceeds with retrieving sensitive time-domain features during fault and no-fault events. The retrieved features are selected based on performance evolution to identify the core features of AC, DC, and IS faults. The data are divided for training and testing to evaluate performance. To assess performance further, noise of 20 dB and 30 dB was added to the data, and the system was also extended. The purpose of this study is to employ AI-based techniques for the safety of emerging hybrid systems. The fast and robust data-driven algorithm can ensure stability and reliability and timely detect fault events and islanding scenarios. In addition, future research will further evaluate the presented algorithm utilizing real-world data and hardware scenarios.

7. Conclusions

In this paper, we developed a data-driven coordination algorithm for the recognition, categorization, and location of faults in the hybrid AC/DC transmission system. The fault characteristics were analyzed using formulated fault current and voltage equations and retrieved data using derived features. The data-driven coordination algorithm was developed using training data and verified using unseen datasets considering various case studies created in MATLAB. The proposed algorithm has detected, classified, and traced the position of line faults. The algorithm was trained with 70% of the dataset and tested with

unseen test data (30%), allowing us to assess its performance. The algorithm's effectiveness was assessed using performance metrics and compared with existing algorithms. The proposed algorithm has detected faults with 99.69% accuracy and recognized faults with 99.62% accuracy. The proposed algorithm was further verified using noisy data and an extended test system. The algorithm has shown good performance in the coordination of AC/DC faults without any communication channel and threshold criteria. Hence, the proposed algorithm can be utilized to ensure the stability and reliability of hybrid protection lines. In the future, a thorough study of hybrid networks and real-time implementation of the proposed algorithm will be conducted to ensure the algorithm's applicability to real-world scenarios.

Author Contributions: Conceptualization, A.M. and A.H.; methodology, A.M.; software, A.M.; validation, A.M., S.J.U.H. and Z.H.; formal analysis, A.M.; investigation, S.J.U.H.; resources, H.-Y.K.; data curation, Z.H.; writing—original draft preparation, A.M.; writing—review and editing, H.-Y.K.; visualization, S.J.U.H.; supervision, A.H.; project administration, H.-Y.K.; funding acquisition, A.M. All authors have read and agreed to the published version of the manuscript.

Funding: This work was supported by the Korea Institute of Energy Technology Evaluation and Planning (KETEP) and the Ministry of Trade, Industry & Energy (MOTIE) of the Republic of Korea (No. 20225500000110).

Data Availability Statement: The data presented in this study is available on request from the corresponding author.

Conflicts of Interest: The authors declare no conflict of interest.

Appendix A

Table A1. Test system specifications.

Equipment	Parameters	Ratings
Generation End	Nominal power	4200 MVA
	Voltage	13.8 kV
	Load	200 MW
	Frequency	60 Hz
Receiving End	X/R ratio	10
	Short-circuit level	20 GVA
	Voltage	765 kV
Transformer	Voltage rating	13.8 kV/765 kV
AC Transmission Line	R1 (Ω/km)	0.01165
	R0 (Ω/km)	0.2676
	L1 (mH/km)	0.8679
	L0 (mH/km)	3.008
	C1 (nF/km)	13.41
	C0 (nF/km)	8.57
DC Transmission Line	R (Ω/km)	0.015
	L (mH/km)	0.792
	C (nF/km)	14.4
Converters/Inverters	Neutral clamped VSC	IGBT/Diodes
AC Side Station	Yg-D transformer	765 kV/230 kV
	AC filter	40 Mvar
	Converter reactor	0.15 p.u
DC Side Station	DC capacitors	7.00×10^{-5}
	DC filters	1.20×10^{-5}
	Smoothing reactors (RL)	R = 0.0251 ohm
		L = 8×10^{-3} H

References

1. Qiao, J.; Zou, J.; Zhang, J.; Lu, Y.; Lee, J.; Ju, M.-N. Space-Time Pattern of Ion Flow Under AC/DC Hybrid Overhead Lines and Its Application. *IEEE Trans. Power Deliv.* **2017**, *33*, 2226–2235. [CrossRef]
2. Tang, J.; Zeng, R.; Ma, H.; He, J.; Zhao, J.; Li, X.; Wang, Q. Analysis of Electromagnetic Interference on DC Line from Parallel AC Line in Close Proximity. *IEEE Trans. Power Deliv.* **2007**, *22*, 2401–2408. [CrossRef]
3. Hussain, A.; Arif, S.M.; Aslam, M. Emerging renewable and sustainable energy technologies: State of the art. *Renew. Sustain. Energy Rev.* **2017**, *71*, 12–28. [CrossRef]
4. Asif, M.; Lee, H.-Y.; Park, K.-H.; Lee, B.-W. Influence of Placement of Overhead Ground Wires on Steady State Induction in AC-DC Hybrid Transmission Corridor. *IEEE Trans. Power Deliv.* **2018**, *33*, 2999–3008. [CrossRef]
5. Hassan, S.J.U.; Mehdi, A.; Haider, Z.; Song, J.-S.; Abraham, A.D.; Shin, G.-S.; Kim, C.-H. Towards medium voltage hybrid AC/DC distribution Systems: Architectural Topologies, planning and operation. *Int. J. Electr. Power Energy Syst.* **2024**, *159*, 110003. [CrossRef]
6. Li, X.; Li, Z.; Guo, L.; Zhu, J.; Wang, Y.; Wang, C. Enhanced Dynamic Stability Control for Low-Inertia Hybrid AC/DC Microgrid with Distributed Energy Storage Systems. *IEEE Access* **2019**, *7*, 91234–91242. [CrossRef]
7. Qiao, J.; Zhang, P.; Zhang, J.; Lu, Y.; Zou, J.; Yuan, J.; Huang, S. An Iterative Flux Tracing Method Without Deutsch Assumption for Ion-Flow Field of AC/DC Hybrid Transmission Lines. *IEEE Trans. Magn.* **2018**, *54*, 1–4. [CrossRef]
8. Rahman, H.; Khan, B.H. Power Upgrading of Transmission Line by Combining AC–DC Transmission. *IEEE Trans. Power Syst.* **2007**, *22*, 459–466. [CrossRef]
9. Kizilcay, M.; Agdemir, A.; Losing, M. Interaction of a HVDC System with 400-kV AC Systems on the Same Tower. In Proceedings of the International Conference on Power System Transient, Kyoto, Japan, 3–6 June 2009; pp. 3–6.
10. Nazarcik, T.; Muzik, V. Modelling of the mutual influence of the parallel AC/DC circuits on the hybrid power transmission line. In Proceedings of the 2018 IEEE Conference of Russian Young Researchers in Electrical and Electronic Engineering (EIConRus), Moscow and St. Petersburg, Russia, 29 January–1 February 2018; pp. 731–736.
11. Mehdi, A.; Kim, C.-H.; Hussain, A.; Kim, J.-S.; Hassan, S.J.U. A Comprehensive Review of Auto-Reclosing Schemes in AC, DC, and Hybrid (AC/DC) Transmission Lines. *IEEE Access* **2021**, *9*, 74325–74342. [CrossRef]
12. Cairoli, P.; Kondratiev, I.; Dougal, R.A. Coordinated Control of the Bus Tie Switches and Power Supply Converters for Fault Protection in DC Microgrids. *IEEE Trans. Power Electron.* **2013**, *28*, 2037–2047. [CrossRef]
13. Ma, J.; Kang, J.; Huang, W.; Wang, Z.; Cheng, P. An AC line pilot protection scheme for AC/DC hybrid system based on composite mode power difference. *Int. J. Electr. Power Energy Syst.* **2022**, *137*, 107834. [CrossRef]
14. Ma, J.; Kang, J.; Zhou, Y.; Cheng, P.; Phadke, A.G. A Novel Pilot Protection Scheme for AC Line Connected to LCC-HVDC Inverter Based on Composite-Mode Model. *IEEE Trans. Power Deliv.* **2021**, *37*, 1627–1639. [CrossRef]
15. Xue, S.; Lu, J.; Liu, C.; Sun, Y.; Liu, B.; Gu, C. A Novel Single-Terminal Fault Location Method for AC Transmission Lines in a MMC-HVDC-Based AC/DC Hybrid System. *Energies* **2018**, *11*, 2066. [CrossRef]
16. Liu, Y.; Lin, Z.; Xiahou, K.; Lin, Y.; Wu, Q.H. Equivalent hamiltonian equations modelling and energy function construction for MMC-HVDC in Hybrid AC/DC power systems. *CSEE J. Power Energy Syst.* **2020**, *7*, 821–831. [CrossRef]
17. Dong, X.; Guan, E.; Jing, L.; Wang, H.; Mirsaeidi, S. Simulation and analysis of cascading faults in hybrid AC/DC power grids. *Int. J. Electr. Power Energy Syst.* **2020**, *115*, 105492. [CrossRef]
18. Mirsaeidi, S.; Dong, X. An Integrated Control and Protection Scheme to Inhibit Blackouts Caused by Cascading Fault in Large-Scale Hybrid AC/DC Power Grids. *IEEE Trans. Power Electron.* **2018**, *34*, 7278–7291. [CrossRef]
19. Saha, M.M.; Hoidalen, H.K.; Torres-Olguin, R. A Simulation Model for Evaluation of Intersystem Fault in a Hybrid AC/DC Power System and its impact on the Protection System. In Proceedings of the 2019 Modern Electric Power Systems (MEPS), Wroclaw, Poland, 9–12 September 2019; pp. 1–6. [CrossRef]
20. Prommetta, J.; Schindler, J.; Jaeger, J.; Keil, T.; Butterer, C.; Ebner, G. Protection Coordination of AC/DC Intersystem Faults in Hybrid Transmission Grids. *IEEE Trans. Power Deliv.* **2020**, *35*, 2896–2904. [CrossRef]
21. Melath, G.; Rangarajan, S.; Agarwal, V. A Novel Control Scheme for Enhancing the Transient Performance of an Islanded Hybrid AC–DC Microgrid. *IEEE Trans. Power Electron.* **2019**, *34*, 9644–9654. [CrossRef]
22. AsghariGovar, S.; Seyedi, H. A Novel Transfer Matrix-Based Approach for Pilot Protection of Hybrid Transmission Lines Considering HIF Location. *IEEE Trans. Power Deliv.* **2020**, *35*, 1749–1757. [CrossRef]
23. Zhang, G.; Jing, L.; Liu, M.; Wang, B.; Dong, X. A novel directional element for high voltage hybrid AC/DC power system. In Proceedings of the2018 China International Conference on Electricity Distribution (CICED), Tianjin, China, 17–19 September 2018; pp. 1137–1141. [CrossRef]
24. Ebner, G.; Döring, D.; Schettler, F.; Würflinger, K.; Zeller, M. Fault handling at hybrid high-voltage AC/DC transmission lines with VSC converters. *IEEE Trans. Power Deliv.* **2017**, *33*, 901–908. [CrossRef]
25. Jasim, A.M.; Jasim, B.H.; Neagu, B.-C.; Alhasnawi, B.N. Coordination Control of a Hybrid AC/DC Smart Microgrid with Online Fault Detection, Diagnostics, and Localization Using Artificial Neural Networks. *Electronics* **2022**, *12*, 187. [CrossRef]

26. Tamrakar, A.K.; Koley, E. A SVM based fault detection and section identification scheme for a hybrid AC/HVDC transmission line with wind farm integration. In Proceedings of the 2020 IEEE First International Conference on Smart Technologies for Power, Energy and Control (STPEC), Nagpur, India, 25–26 September 2020; pp. 1–5.
27. Naik, S.; Koley, E. Fault detection and classification scheme using KNN for AC/HVDC transmission lines. In Proceedings of the 2019 International Conference on Communication and Electronics Systems (ICCES), Coimbatore, India, 17–19 July 2019; pp. 1131–1135.
28. Livani, H.; Evrenosoglu, C.Y. A Machine Learning and Wavelet-Based Fault Location Method for Hybrid Transmission Lines. *IEEE Trans. Smart Grid* **2014**, *5*, 51–59. [CrossRef]
29. Duan, J.; Yi, Z.; Shi, D.; Lin, C.; Lu, X.; Wang, Z. Reinforcement-Learning-Based Optimal Control of Hybrid Energy Storage Systems in Hybrid AC–DC Microgrids. *IEEE Trans. Ind. Inform.* **2019**, *15*, 5355–5364. [CrossRef]
30. Jawad, R.S.; Abid, H. HVDC Fault Detection and Classification with Artificial Neural Network Based on ACO-DWT Method. *Energies* **2023**, *16*, 1064. [CrossRef]
31. Yousaf, M.Z.; Khalid, S.; Tahir, M.F.; Tzes, A.; Raza, A. A novel dc fault protection scheme based on intelligent network for meshed dc grids. *Int. J. Electr. Power Energy Syst.* **2023**, *154*, 109423. [CrossRef]
32. Wang, T.; Zhang, C.; Hao, Z.; Monti, A.; Ponci, F. Data-driven fault detection and isolation in DC microgrids without prior fault data: A transfer learning approach. *Appl. Energy* **2023**, *336*, 120708. [CrossRef]
33. Daisy, M.; Aliabadi, M.H.; Javadi, S.; Naimi, H.M. Data-driven fault location approach in AC/DC microgrids based on fault voltage and current differences. *Sustain. Energy, Grids Netw.* **2023**, *36*, 101235. [CrossRef]
34. Wu, S.; He, B.; Meng, F.; Liu, Y.; Lin, X.; Dai, W.; Wei, Y.; Wang, S.; Zhang, D. Machine learning-based single-phase ground fault identification strategy for AC-DC transmission lines. *Electr. Power Syst. Res.* **2023**, *223*, 109538. [CrossRef]
35. Cano, A.; Arévalo, P.; Benavides, D.; Jurado, F. Integrating discrete wavelet transform with neural networks and machine learning for fault detection in microgrids. *Int. J. Electr. Power Energy Syst.* **2023**, *155*, 109616. [CrossRef]
36. Bhargav, R.; Gupta, C.P.; Bhalja, B.R. Unified Impedance-Based Relaying Scheme for the Protection of Hybrid AC/DC Microgrid. *IEEE Trans. Smart Grid* **2021**, *13*, 913–927. [CrossRef]
37. Mehdi, A.; Hassan, S.U.; Haider, Z.; Arefaynie, A.D.; Song, J.-S.; Kim, C.-H. A systematic review of fault characteristics and protection schemes in hybrid AC/DC networks: Challenges and future directions. *Energy Rep.* **2024**, *12*, 120–142. [CrossRef]
38. Ademi, S.; Tzelepis, D.; Dysko, A.; Subramanian, S.; Ha, H. Fault current characterisation in VSC-based HVDC systems. In Proceedings of the 13th International Conference on Development in Power System Protection 2016 (DPSP), Edinburgh, UK, 7–10 March 2016. [CrossRef]
39. Keller, J.; Kroposki, B. *Understanding Fault Characteristics of Inverter-Based Distributed Energy Resources*; National Renewable Energy Lab. (NREL): Golden, CO, USA, 2010.
40. Hussain, A.; Kim, C.; Admasie, S. An intelligent islanding detection of distribution networks with synchronous machine DG using ensemble learning and canonical methods. *IET Gener. Transm. Distrib.* **2021**, *15*, 3242–3255. [CrossRef]
41. Chen, Z.; Han, F.; Wu, L.; Yu, J.; Cheng, S.; Lin, P.; Chen, H. Random forest based intelligent fault diagnosis for PV arrays using array voltage and string currents. *Energy Convers. Manag.* **2018**, *178*, 250–264. [CrossRef]
42. Tibshirani, S.; Friedman, H. *The Elements of Statistical Learning: Data Mining, Inference, and Prediction*, 2nd ed.; CiNii: New York, NY, USA, 2009; Volume 745, ISBN 0172-7397.
43. Natekin, A.; Knoll, A. Gradient boosting machines, a tutorial. *Front. Neurorobot.* **2013**, *7*, 21. [CrossRef]
44. Hussain, A.; Kim, C.-H.; Mehdi, A. A Comprehensive Review of Intelligent Islanding Schemes and Feature Selection Techniques for Distributed Generation System. *IEEE Access* **2021**, *9*, 146603–146624. [CrossRef]